Journal of Electrical Engineering, Vol. 77, No. 1, 2026, pp. 77-88
https://reference-global.com/journal/JEE

Adaptive model-free sliding mode control for boost converter with flexibility to varying operating conditions

Abbes Kihal[1], Chems Eddine Boudjedir[2], Billel Talbi[3], Abdeslem Sahli[3], Abdelbasset Krama[4]

DC-DC boost converter (BC) is widely used in renewable energy systems and electric vehicles due to their high efficiency, compactness, and strong dynamic performance. However, input voltage fluctuations and parameter variations make maintaining stable operation challenging. Sliding Mode Control (SMC) offers high robustness but relies heavily on accurate system models, making it sensitive to uncertainties. In contrast, Model-Free Control (MFC) based on the ultra-local model (ULM) provides simplicity and robustness by estimating system behaviour in real time from input-output measurements. MFC is effective for minimum-phase systems but struggles with non-minimum-phase systems like BCs. To overcome this, an adaptive MFC-SMC (AMF-SMC) scheme is proposed, combining MFC and SMC principles. The approach uses ULM with a time-delay estimation (TDE) technique and an adaptive gain mechanism to enhance precision and responsiveness. Lyapunov analysis confirms uniform ultimate boundedness of the sliding surface. Comparative experiments demonstrate the proposed controller's superior robustness, high accuracy, and chattering-free operation.

Keywords: DC-DC boost converter, Model-Free control, Time-delay estimation, Adaptive sliding mode control.

1 Introduction

The ability of DC-DC boost converter (BC) to elevate an input voltage to a higher level makes it vital in numerous applications, including consumer electronics, electric vehicles (EVs), renewable energy systems (RESs), computer systems, robotics [1]. The BC steps up voltage by switching between two circuit modes, storing energy during the ON phase and releasing it during the OFF phase. This process causes a phase lag, known as non-minimum-phase behaviour, due to a right-half-plane zero (RHPZ) in the control-to-output voltage path [2]. The increasing demand for accurate and stable voltage regulation in the presence of varying load and input conditions has prompted the development of more robust and adaptive control strategies to ensure reliable and efficient performance. Consequently, various control methods have been developed and refined over time to address these dynamic requirements [3-12].

At present, the linear proportional-integral (PI) control remains the most widely investigated scheme for the BC applications [3]. However, this classical approach often faces limitations when dealing with input and load disturbances, as it lacks adaptability and relies on fixed parameters. To address these shortcomings, several advanced nonlinear control techniques have been developed for DC-DC converters, including sliding mode control (SMC) [4-6], and model predictive control (MPC) [7-8], both recognized for their improved robustness. Nevertheless, beyond their well-known limitations such as chattering in SMC and variable switching frequency in MPC, these methods inherently rely on an accurate mathematical model of the system, which can significantly limit their performance in real-world applications, where uncertainties, parameter variations, and dynamic changes are common. As a result, their effectiveness may be compromised, and the overall implementation becomes more complex and less adaptable. To overcome these issues, adaptive controllers [9-11] and iterative learning controllers [12] have been introduced to better handle for the nonlinear and coupled dynamics of the BC, thereby enhancing tracking performance. However, their effectiveness is still constrained by the reliance on mathematical models and the limited availability of precise knowledge about system dynamics and parameters.

[1] Department of Automatic, Faculty of Electrical Engineering, University of Science and Technology Houari Boumediene (USTHB), Algiers 16111, Algeria
[2] LRPE Laboratory, University of science and Technology Houari Boumediene (USTHB), B.P 32, El Alia 16111 Bab Ezzouar, Algiers, Algeria
[3] ETA Laboratory, Department of Electronics, University Mohamed El Bachir El Ibrahimi of Bordj Bou Arreridj, El Anceur 34030, Algeria
[4] Qatar Environment and Energy Research Institute, Hamad Bin Khalifa University, Doha, Qatar
akihal@usthb.dz, chemseddine.boudjedir@usthb.edu.dz, billel.talbi@univ-bba.dz, abdeslem.sahli@univ-bba.dz, akrama@hbku.edu.qa

https://doi.org/10.2478/jee-2026-0008, Print (till 2015) ISSN 1335-3632, On-line ISSN 1339-309X

In response to these limitations, model-free control (MFC) methods have been developed to ensure robust performance in systems affected by disturbances and modelling uncertainties [13-26]. Numerous studies have explored MFC strategies based on predictive control (MF-PC) and sliding mode control (MF-SMC). In [13], an MF-PC approach was proposed for permanent magnet synchronous motor drives, where the nonlinearities and uncertainties introduced by the motor and inverter were effectively addressed using an algebraic estimation (AE) technique. Furthermore, [14] and [15] introduced MF-PC schemes incorporating an extended state observer (ESO) to improve disturbance estimation. In [16], a hybrid PC-ESO was proposed for the BC to enhance disturbance rejection capability and reduce sensitivity to measurement noise. One of the prominent techniques in MFC is the ultra-local model (ULM), which approximates the system's input–output behaviour locally without requiring an explicit model of the system dynamics [17]. In this approach, the unknown system dynamics and external disturbances are lumped into a single term, which is estimated in real-time using only the system input and output, without the need to distinguish between the sources of uncertainty [18, 19]. For DC-DC converters, this approach was applied in [20] to develop an MF-PC strategy for an interleaved BC, where AE was used to handle current balancing and parameter uncertainties. However, the estimation of internal dynamics and disturbances in the ULM framework typically relies on algebraic methods, which can involve complex and computationally demanding calculations [17]. To address this limitation, time-delay estimation (TDE) has been adopted as a practical alternative [21]. TDE offers a straightforward and robust approach for estimating total disturbances, effectively reducing implementation complexity while preserving the advantages of MFC. Nevertheless, in the TDE-based control, estimation errors are inevitable due to the finite sampling time and the approximation involved in using delayed signals to represent system dynamics. A common strategy to compensate for these errors is to introduce a robust control term, such as a SMC, which is well known for its ability to handle bounded uncertainties and external disturbances. In [22], a nonlinear terminal SMC (NTSMC) was integrated into the TDE-PD framework as a compensator. However, this method assumes that the upper bound of the estimation error is known, a condition that is often difficult to guarantee in practical scenarios. Consequently, the switching gain, which must exceed this bound to ensure stability, is typically chosen conservatively large, leading to pronounced chattering. Another scheme was developed for quadrotor control in [23]. Whereas, to further improve tracking convergence and reduce chattering, an adaptive model-free sliding mode controller integrated with TDE was proposed for the trajectory tracking of robotic manipulators [24]. In contrast, applications of MF-SMC in power converter systems remain scarce. A notable example is presented in [25], where a sliding mode observer (SMO) was employed within the ULM framework to estimate unknown dynamics in permanent magnet synchronous motor (PMSM) drives. However, to the best of our knowledge, no existing studies have yet explored the implementation of adaptive ULM-based SMC strategies for DC-DC converters.

To address this research gap, this paper proposes an adaptive MF-SMC (AMF-SMC) scheme with TDE based on ULM method for the BC. The proposed method aims to enhance tracking performance and mitigate chattering under model uncertainties and load/input disturbances, while preserving implementtation simplicity and robustness. In this framework, the TDE technique is employed to estimate the unknown dynamics exhibited by the ULM approach. Subsequently, a SMC is incorporated to ensure the robustness of the overall control strategy. Given the non-minimum-phase nature of the BC, a global sliding surface is meticulously designed to ensure system stability and effective output regulation. Furthermore, an adaptive sliding gain is proposed to enhance tracking accuracy. The dynamic gain is tuned based on the thickness of the desired dynamic injection layer, ensuring that the tracking error remains bounded. The stability of the closed-loop system and the uniform ultimate boundedness of the sliding surface are proven using Lyapunov method. Additionally, the approach does not necessitate prior knowledge of the upper bound of the lumped disturbances. The effectiveness of the proposed control scheme under various operating conditions is validated through experimental testing, demonstrating superior performance in comparison to both the conventional PID control scheme and the integral sliding mode scheme (ISMC).

The remainder of this paper is organized as follows. Section 2 introduces the system description, preliminaries, and associated control objectives. In Section 3, the proposed AMF-SMC with TDE is presented, along with a detailed design procedure and stability analysis. Experimental validation is provided in Section 4. Finally, the conclusions are drawn in Section 5.

2 System description, preliminaries, and control objectives

As illustrated in Fig. 1, the system under study is a BC, which comprises the following components: an inductor L for energy storage, a freewheeling diode D to direct current flow, a switch S (typically an IGBT) controlled by a PWM signal, an output capacitor C

for voltage smoothing, and a resistive load R. The variables $[v_{in}(t), v_{out}(t), i_L(t)]$ represent the measured input voltage, output voltage, and inductor current, respectively.

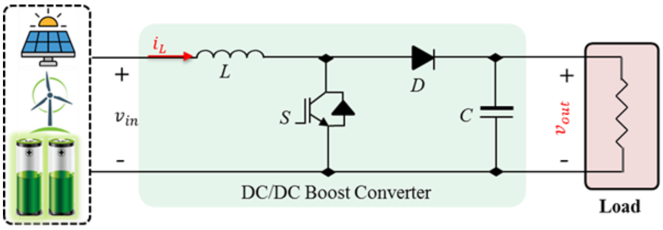

Fig. 1. DC-DC BC architecture

The dynamic model of the BC over a switching period can be formulated using the state-space averaging technique as:

$$\underbrace{\begin{pmatrix}\dot{x}_1(t)\\ \dot{x}_2(t)\end{pmatrix}}_{\dot{x}} = \underbrace{\begin{bmatrix}0 & -\frac{1}{L}\\ \frac{1}{C} & -\frac{1}{RC}\end{bmatrix}}_{A}\begin{pmatrix}x_1(t)\\ x_2(t)\end{pmatrix} + \underbrace{\begin{pmatrix}\frac{x_2(t)}{L}\\ -\frac{x_1(t)}{C}\end{pmatrix}}_{B} u(t) + \underbrace{\begin{pmatrix}\frac{v_{in}(t)}{L}\\ 0\end{pmatrix}}_{d} \qquad (1)$$

where $[x_1(t) \quad x_2(t)]^T = [i_L(t) \quad v_{out}(t)]^T$ is the state vector, $u(t)$ is the input control (duty cycle), and d is the external disturbance term.

2.1 ULM concept

The ULM strategy substitutes the unknown system dynamics with a simplified local input-output representation of the form [17]:

$$y^{(n)}(t) = F(t) + \alpha\, u(t) \qquad (2)$$

where $y(t)$ represents the system output, n indicates the orders of derivative, while $F(t)$ signifies the unknown dynamics and external disturbances, which is continuously updated. The nonphysical coefficient α is designed such that both sides of Eqn. (2) are of the same magnitude.

Assuming $n = 1$, the control law using intelligent controllers can be expressed in the following form [17]:

$$u(t) = \frac{1}{\alpha}\left[-\hat{F}(t) + \dot{y}_{ref}(t) + \Theta(\mathrm{e}(t))\right] \qquad (3)$$

where $e(t)$ is the tracking error between the desired output $y_{ref}(t)$ and the measured output $y(t)$, $\hat{F}(t)$ is the estimated value of $F(t)$, and $\Theta(\mathrm{e}(t))$ is a causal or non-anticipative, functional of $e(t)$, i.e., $\Theta(e(t))$ depends only on the past and the present.

2.2 TDE concept

Accurate estimation of $F(t)$ is essential for effective MFC. Instead of relying on complex algebraic identification methods [13-15], the TDE technique [26, 27] is adopted. Assuming a sufficiently small-time delay T_d, a valid approximation of $F(t)$ can be derived based on Eqn. (2).

$$\begin{aligned} F(t) \approx \hat{F}(t) &= F(t - T_d) \\ &= \dot{y}(t - T_d) - \alpha\, u(t - T_d) \end{aligned} \qquad (4)$$

Here, T_d represents the delay time and $\hat{F}(t)$ denotes the estimated value of $F(t)$. In practical implementations, T_d is typically selected to be equal to the sampling period.

Assumption 1: The time delay estimation error is bounded as follows:

$$\left|\hat{F}(t) - F(t)\right| \le \varepsilon \qquad (5)$$

where ε is an unknown positive constant.

Remark 1: This *assumption* is reasonable and has been adopted in previous works [26, 27]. In our case, the estimation error is given by:

$$\begin{aligned} \hat{F}(t) - F(t) = \dot{x}_2(t - T_d) - \dot{x}_2(t) \\ + \alpha\,[u(t) - u(t - T_d)] \end{aligned} \qquad (6)$$

Therefore, for a sufficiently small-time delay T_d it is well-justified to assume that $|\dot{x}_2(t - T_d) - \dot{x}_2(t)|$, and $|u(t) - u(t - T_d)|$ | remain bounded. Moreover, the control law does not require knowledge of this bound.

2.3 Control objectives

The standard ULM concept mentioned in Eqn. (2) is derived under the assumption that the system exhibits minimum-phase (MP) behavior [17]. However, controlling a BC remains challenging due to its inherently non-minimum-phase nature. In particular, relying solely on the output voltage error for control can lead to performance degradation and potential instability, as the output voltage initially responds in the opposite direction to changes in the control input.

This paper aims to develop a control strategy that integrates SMC within the ULM framework to effectively address the non-minimum-phase behavior of the BC, ensuring stable tracking performance by designing a sliding surface that includes both the output voltage and the inductor current as MP output. To further enhance robustness and mitigate chattering effects typically associated with MFC-SMC, an adaptive gain mechanism should be also designed. Furthermore, integrating TDE to estimate the unknown dynamic term $F(t)$, simplifyies the implementation while preserving the robustness and model-free nature of the control law.

3 Suggested AMF-SMC with TDE

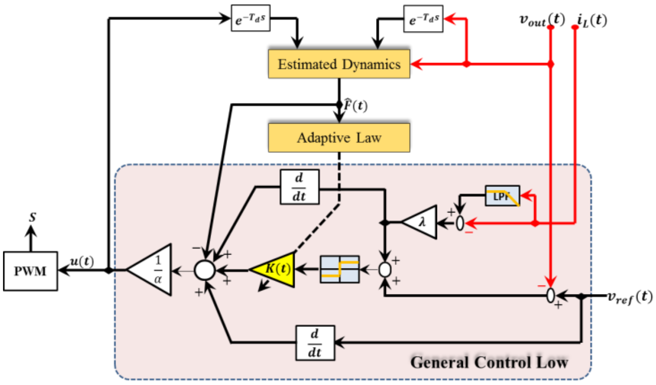

Fig. 2. Block diagram of the proposed AMF-SMC (s is a Laplace variable)

The schematic diagram of suggested AMF-SMC for a BC is mainly composed of three parts: 1) The estimated dynamic uses TDE method to estimate the desired dynamics injection term $\hat{F}(t)$ in real-time. 2) The general control law is designed by incorporating the SMC within ULM framework to increase the tracking performance. 3) The adaptive law is used to automatically adjust the gain $K(t)$ of the general control law gain according to the thickness of the acceptance $\hat{F}(t)$. These parts collectively generate the control input $u(t)$ for PWM stage, as depicted in Fig. 2.

3.1 Control design

For the DC-DC BC, the controller's input is the switching duty cycle $u(t)$, while its output corresponds to the regulated output voltage $x_2(t)$, $(y(t) = x_2(t) = v_{out}(t))$.

Using the relationships in Eqn. (2), $F(t)$ can be formulated as follows:

$$F(t) = \dot{x}_2(t) - \alpha\, u(t) \tag{7}$$

Using Eqn. (4), the estimation of $F(t)$ can be achieved as follows:

$$\hat{F}(t) = F(t - T_d) = \dot{x}_2(t - T_d) - \alpha\, u(t - T_d) \tag{8}$$

The delayed of $\dot{x}_2(t - T_d)$ can be approximated using the following expression:

$$\dot{x}_2(t - T_d) = \frac{x_2(t) - x_2(t - T_d)}{T_s} \tag{9}$$

where T_s is the sampling time.

Substituting Eqn. (9) into Eqn. (8) yields,

$$\hat{F}(t) = \frac{x_2(t) - x_2(t - T_d)}{T_s} - \alpha * u(t - T_d) \tag{10}$$

The TDE technique provides a practical method for estimating unknown system dynamics, but it may not ensure sufficient tracking accuracy when used alone. To enhance the robustness along with reliable tracking performance, it was integrated with SMC.

According to the structure of the BC, the sliding surface was selected as follows:

$$s(t) = \lambda e_1(t) + e_2(t)$$
$$\text{with,} \begin{cases} e_1(t) = x_{1,ref}(t) - x_1(t) \\ e_2(t) = x_{2,ref}(t) - x_2(t) \end{cases} \tag{11}$$

where λ is the sliding surface coefficient, $x_{2,ref}(t)$ represents the desired output voltage, and $x_{1,ref}(t)$ corresponds to the input current reference, which can be estimated using a first-order low-pass filter.

The time derivative of $s(t)$ can be expressed as:

$$\begin{aligned} \dot{s}(t) &= \lambda \dot{e}_1(t) + \dot{e}_2(t) \\ &= \lambda\left(\dot{x}_{1,ref}(t) - \dot{x}_1(t)\right) + \dot{x}_{2,ref}(t) - \dot{x}_2(t) \end{aligned} \tag{12}$$

To provide an ideal sliding motion, the sliding surface and its derivative must converge to zero $\dot{s}(t) = s(t) = 0$:

$$\dot{x}_2(t) = \lambda\left(\dot{x}_{1,ref}(t) - \dot{x}_1(t)\right) + \dot{x}_{2,ref}(t) \tag{13}$$

From Eqn. (10), when T_d is sufficiently small, $\hat{F}(t) \approx F(t)$. By substituting Eqn. (13) into Eqn. (7), we obtain the following expression:

$$\begin{aligned} \hat{F}(t) + \alpha\, u(t) = \lambda\big(&\dot{x}_{1,ref}(t) - \dot{x}_1(t)\big) \\ &+ \dot{x}_{2,ref}(t) \end{aligned} \tag{14}$$

The proposed control law is defined as:

$$\begin{aligned} u(t) = \frac{1}{\alpha}\Big[&-\hat{F}(t) + \lambda\left(\dot{x}_{1,ref}(t) - \dot{x}_1(t)\right) \\ &+ \dot{x}_{2,ref}(t) + K(t)\text{sign}(s(t))\Big] \end{aligned} \tag{15}$$

Where, the term $[K(t).\text{sign}(s(t))]$ represents the discontinuous part of the control law, with $K(t)$ denoting the adaptive gain.

Remark 2: To enable practical implementation, it is preferable to use a first-order derivative low-pass filter for estimating $\dot{x}_{2,ref}$.

Remark 3: It should be noted that a constant sliding gain $K(t)$ may lead to performance degradation, particularly under varying operating conditions such as changes in input voltage or load disturbances. This limitation reduces the adaptability and robustness of the proposed control scheme. To overcome this issue and mitigate chattering, a dynamic gain adaptation law is introduced, as defined in Eqn. (16). This mechanism enables real-time adjustment of the controller gain in response to system variations, thereby enhancing robustness and improving overall control performance.

The time-varying gain $K(t)$ is given by:

$$K(t) = \mu + \rho\left|\hat{F}(t)\right| \quad (16)$$

where μ and ρ are positive constant gains.

3.2 Convergence analysis

Proposition: Consider the dynamics of BC described by Eqn. (1), under *assumption 1*. If the control law Eqn. (15) is applied then closed-loop system is stable, and the sliding surface is uniformly ultimately bounded (UUB) as given by:

$$|s(t)| < \sqrt{s^2(0) + 2s_{max}^2} \quad (17)$$

with $s_{max} = -\frac{\varepsilon}{K(t)} + 1$.

Proof: Consider the following Lyapunov candidate function:

$$V(t) = \frac{1}{2}s^2(t) + \int_0^t K(\tau)d\tau \quad (18)$$

The time derivative of $V(t)$ is given by:

$$\dot{V}(t) = s(t)\dot{s}(t) + K(t) \quad (19)$$

Hence,

$$\begin{aligned}\dot{V}(t) &= s(t)\dot{s}(t) + K(t) \\ &= s\left[\dot{x}_{2,ref}(t) - \dot{x}_2(t) + \lambda\left(\dot{x}_{1,ref}(t) - \dot{x}_1(t)\right)\right] + K(t)\end{aligned} \quad (20)$$

Substituting the expression of "$\dot{x}_2(t)$" from Eqn. (7) into Eqn. (20) yields:

$$\begin{aligned}\dot{V}(t) = s(t)\big[\dot{x}_{2,ref}(t) - F(t) - \alpha u(t) \\ + \lambda\left(\dot{x}_{1,ref}(t) - \dot{x}_1(t)\right)\big] \\ + K(t)\end{aligned} \quad (21)$$

By inserting the control expression in Eqn. (15) into Eqn. (21), we get:

$$\begin{aligned}\dot{V}(t) = s(t)[\dot{x}_{2,ref}(t) - F(t) - \dot{x}_{2,ref}(t) \\ + \lambda\left(\dot{x}_{1,ref}(t) - \dot{x}_1(t)\right) + \hat{F}(t) \\ - \lambda\left(\dot{x}_{1,ref}(t) - \dot{x}_1(t)\right) \\ - K(t)\text{sign}(s(t)))] + K(t)\end{aligned} \quad (22)$$

Simplifying Eqn. (22) yields:

$$\begin{aligned}\dot{V}(t) = s\left[\hat{F}(t) - F(t) - K(t)\text{sign}(s(t))\right] \\ + K(t)\end{aligned} \quad (23)$$

Using *assumption 1*, we can get:

$$\dot{V}(t) \le |s(t)|[\varepsilon - K(t)] + K(t)|s(t)||s(t)|^{-1} \quad (24)$$

Hence,

$$\dot{V}(t) \le |s(t)|(\varepsilon + K(t)(|s(t)|^{-1} - 1)) \quad (25)$$

Therefore, when $|s(t)| \ge -\frac{\varepsilon}{K(t)} + 1$, we have $\dot{V}(t) \le 0$. In this case, $V(t)$ decreases and the sliding variable s enters the set:

$$S = \left\{s \in R \mid |s(t)| < s_{max} = -\frac{\varepsilon}{K(t)} + 1\right\} \quad (26)$$

Since $\dot{V}(t)$ is indefinite within this set, the variable s may exit the set S, i.e., $|s(t)| \ge -\frac{\varepsilon}{K(t)} + 1$. In this case, $\dot{V}(t)$ becomes negative again, as shown in Eqn. (25) and the variable s is driven back into the set S.

The upper bound of s can be obtained as follows:

$$\frac{1}{2}s^2(t) \le V(t) \le \frac{1}{2}s^2(t) + \int_0^t K(\tau)d\tau \quad (27)$$

Since $V(t)$ is decreasing, then it follows that, $V(t) \le V(0)$. Therefore,

$$\frac{1}{2}s^2(t) + \int_0^t K(\tau)d\tau \le \frac{1}{2}s^2(0) \quad (28)$$

Hence, the integral term is bounded as:

$$\int_0^t K(\tau)d\tau \le \frac{1}{2}s^2(0) + \frac{1}{2}s_{max}^2 \quad (29)$$

Therefore,

$$\frac{1}{2}s^2(t) \le \frac{1}{2}s^2(0) + s_{max}^2 \quad (30)$$

Finally, we can obtain:

$$|s(t)| \le \sqrt{s^2(0) + 2s_{max}^2} \quad (31)$$

We conclude that $s(t)$ is UUB, and thus, the closed-loop system is stable.

Remark 4: The parameters μ and ρ are tunable design constants that can be selected to ensure fast tracking performance and a reduced upper bound on the sliding variable. Proper tuning of these parameters allows for a favorable trade-off between robustness and chattering attenuation.

4 Experimental results and discussion

A practical experiment, shown in Fig. 3, was conducted to validate the effectiveness of the proposed scheme. The experimental test bench was built around a BC supplied by a programmable power supply to ensure stable operating conditions. The setup contains a Semikron IGBT driver module, a voltage amplification card (5-15 V) for adapting control signals, and ADC/DAC interfaces for bidirectional communication with the dSPACE DS1104 control board. The implemented control schemes were developed using MATLAB/Simulink®. Furthermore, the system was tested under various operating scenarios, including variations in the output voltage reference, dynamic load disturbances, and input voltage disturbances.

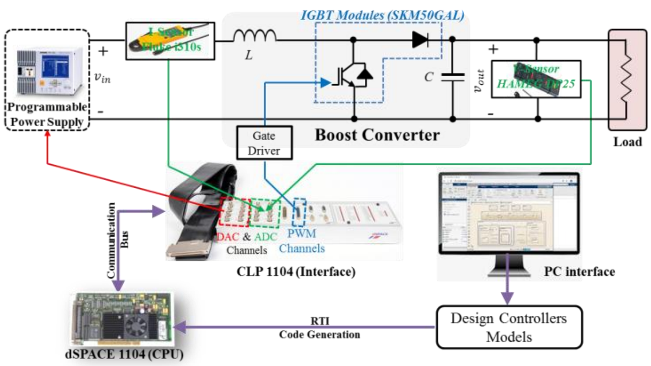

Fig. 3. Schematic representation of the BC experimental setup

The objective was to evaluate the controller's capability to maintain output voltage regulation in the presence of both input-side and output-side disturbances, in line with the application domains of the BC, such as REs and EVs. The nominal parameters of the BC, along with the control settings, are summarized in Tab. 1.

Table 1. Specifications of the BC and control parameters

BC parameters	Nominal values	Control parameters	Nominal values
Input voltage v_{in}	24 V	μ, ρ	1.3, 0.5
Inductance L	1 mH	λ	0.1
Capacitor C	330 μF	α	8000
Resistive load R	50 Ω	Sampling time T_s	0.5×10^{-4}
Switching frequency f_{pwm}	10 kHz	Delay time T_d	0.5×10^{-4}

4.1 Performance analyses under output reference voltage variations

To assess the controller's capability to accurately track the desired reference and maintain voltage regulation, it is crucial to evaluate its dynamic response, stability, and robustness against transients. This is especially important in practical power electronics systems like REs or EVs, where the output voltage requirements can vary during operation.

Scenario 1: Fast change in output reference voltage

Figures 4, 5 and 6 depict the dynamic behavior of the BC under the implemented controllers in response to sudden changes in the output voltage reference. All controllers exhibited adequate steady-state tracking; however, their transient responses showed notable differences.

As depicted in Fig. 4, the PID control scheme presented poorer transient performance, characterized by more distinct overshoot/undershoot and longer settling times relative to both the ISMC and the proposed control schemes. Nevertheless, it is worth noting that the ISMC scheme exhibited stable transient behavior, with no overshoot or undershoot and moderate settling times as shown in Fig. 5.

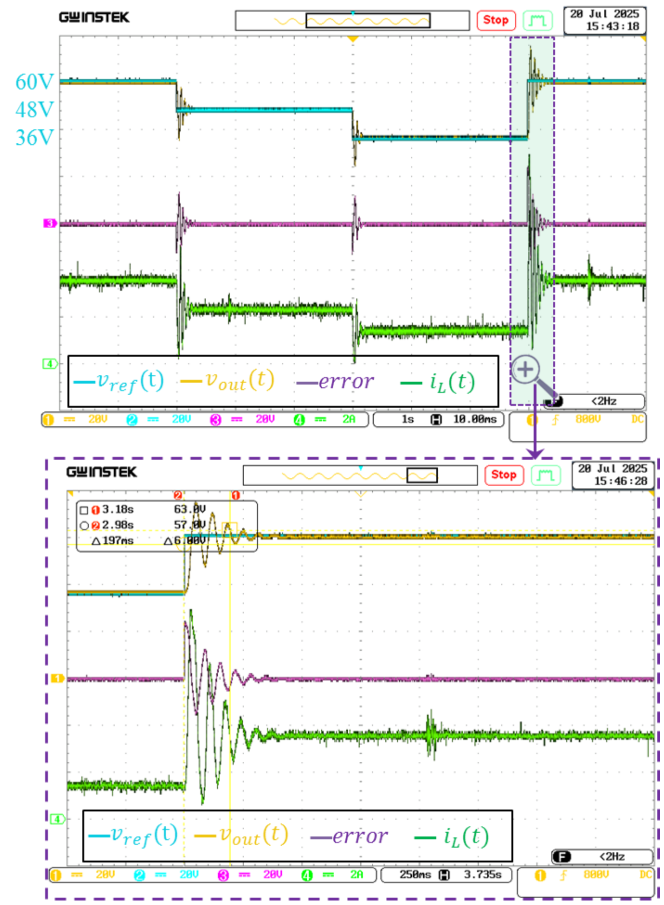

Fig. 4. Experimental results of the PID control scheme under step variations in the output voltage reference

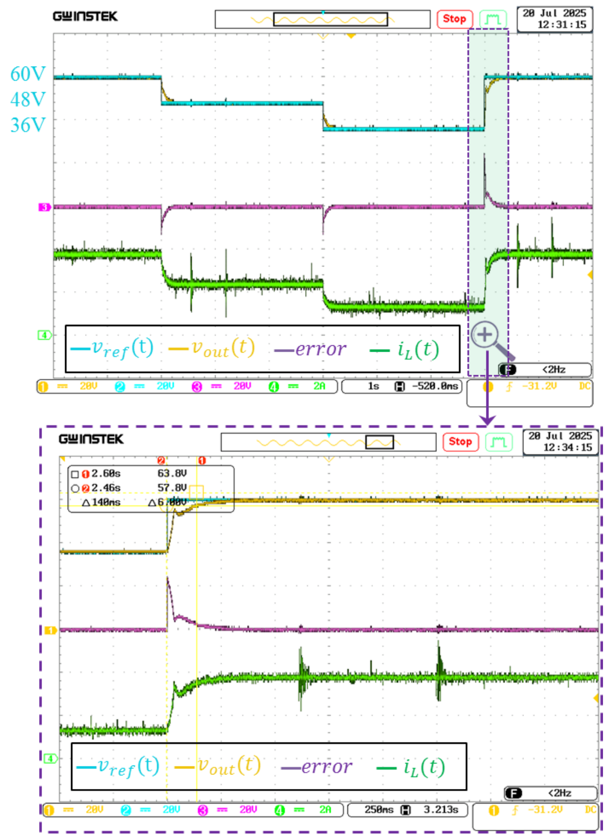

Fig. 5. Experimental results of the ISMC controller scheme under step variations in the output voltage reference

Figure 6 highlights the superiority and ability of the proposed AMF-SMC controller to accurately track the reference, while exhibiting shorter settling times despite sudden changes in the output voltage reference.

Table 2 summarizes the experimental evaluation of the dynamic performance, specifically the settling time of the implemented control schemes in response to sudden changes in the reference voltage.

Table 2. Experimental assessment of control schemes based on settling time (ms) under Scenario 1

Control scheme	From 60 V to 48 V	From 48 V to 36 V	From 36 V to 60 V
PID	120	120	197
ISMC	100	100	140
Proposed	25	25	75

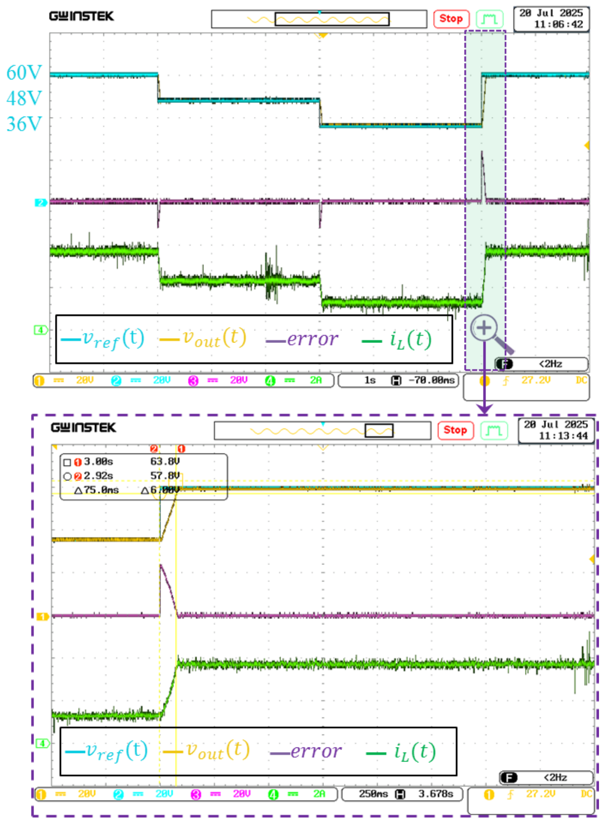

Fig. 6. Experimental results of the proposed scheme under step variations in the output voltage reference

Scenario 2: Gradual change in output reference voltage

To further assess the dynamic tracking capabilities, sinusoidal and triangular reference voltage shapes were applied. These waveforms were intentionally chosen to emulate linearly and smoothly varying setpoints, providing a rigorous evaluation of the controllers' precision and responsiveness in regulating the output voltage.

The experimental results, presented in Figs. 7 and 8, demonstrate the limitations of the PID control scheme in tracking time-varying reference signals, with noticeable lag and tracking errors. The ISMC offered better responsiveness but still suffered from significant steady-state errors under both test scenarios. In contrast, the proposed AMF-SMC controller consistently delivered superior performance; attaining fast transient response and accurate tracking without overshoot or delay due to the adaptive mechanism. These findings approve the effectiveness of the AMF-SMC scheme in applications that demand real-time and precise adaptation to dynamic reference signals.

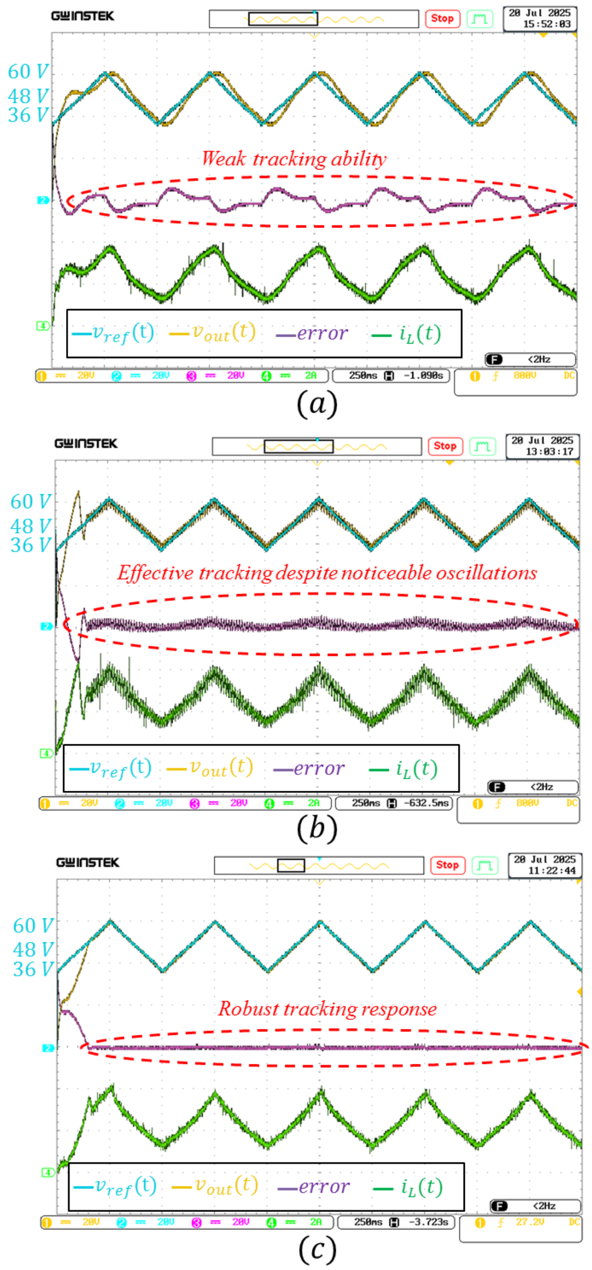

Fig. 7. Experimental results: under triangular reference voltage shapes: (a) PID, (b) ISMC, (c) proposed AMF-SMC

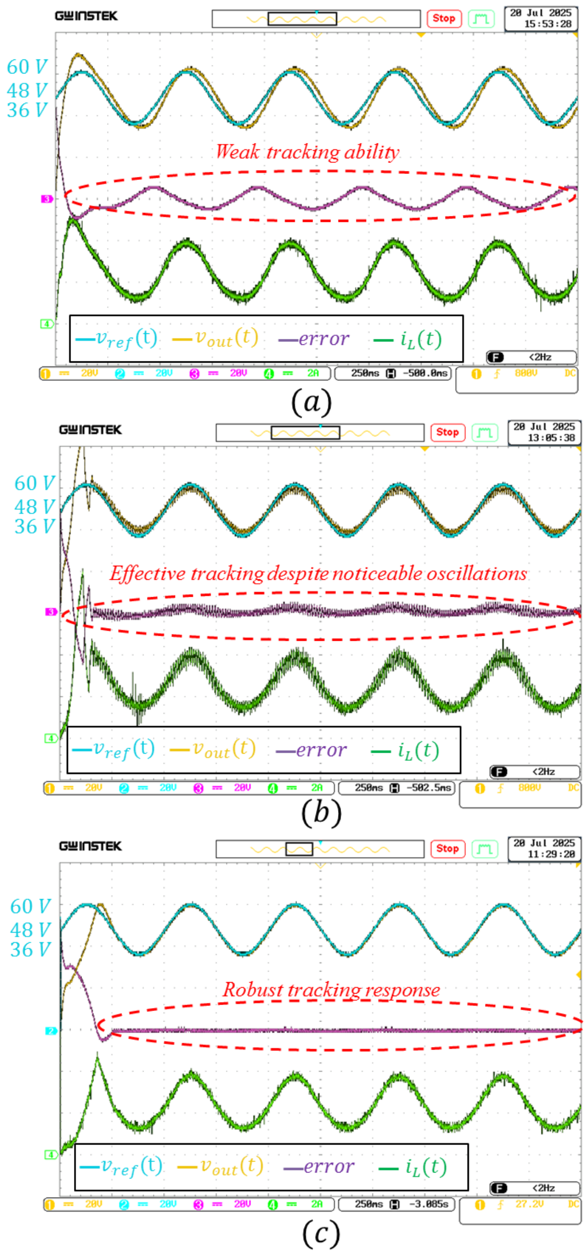

Fig. 8. Experimental results: under sinusoidal reference voltage shapes: (a) PID, (b) ISMC, (c) proposed AMF-SMC

4.2 Performance analyses under load disturbance

In this test scenario, the output voltage reference is fixed at 48 V, while the resistive load ($R = 50\,\Omega$) is decreased by 50% and subsequently returned to its initial value. Figure 9 highlights the performance of the implemented controllers in stabilizing the output voltage under abrupt load changes. The PID control scheme is able to stabilize $v_{out}(t)$ to the reference value, but only after a relatively long transient of about 100 ms, and it displays a peak overshoot/undershoot of approximately 10%. Moreover, the ISMC controller needs around 175 ms to reach the reference value, showing a higher peak overshoot/undershoot of approximately 25%. The proposed AMF-SMC achieves a significantly faster response about 50 ms and limits the peak overshoot/undershoot to around 12%, highlighting superior ability to handle load changes and maintain voltage stability.

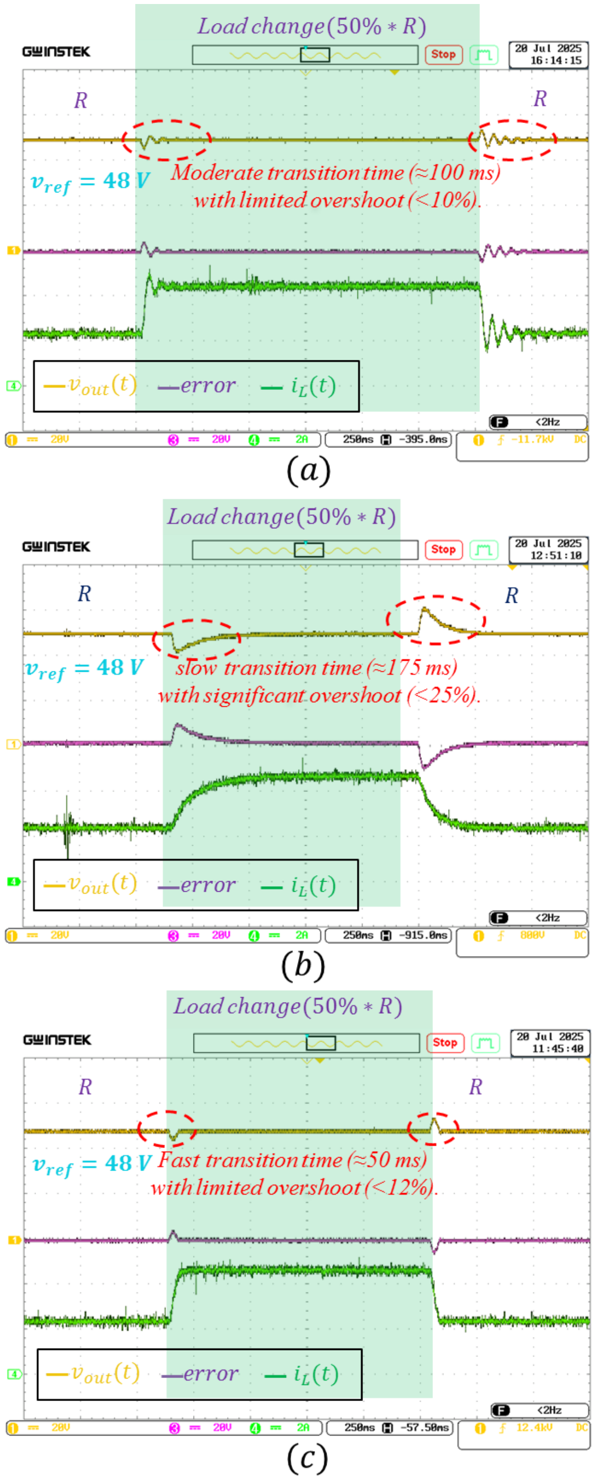

Fig. 9. Experimental results: under step changes in resistive load: (a) PID, (b) ISMC, (c) proposed AMF-SMC

4.3 Performance Analyses under input voltage disturbances

In electric vehicle charging (EVC) systems, the input voltage to the boost converter is typically a rectified sinusoidal waveform derived from the AC mains, exhibiting continuous variation within each cycle. Additionally, when powered by renewable energy sources, the output is weather-dependent and inherently variable. As a result, the control system must ensure robust performance to effectively handle fluctuations in the input voltage v_{in} and maintain a stable output voltage $v_{out}(t)$. To emulate practical and dynamic disturbances, a composite voltage waveform is applied to the input during this experiment scenario. Disturbances, a composite voltage waveform is applied to the input during this experiment scenario.

As illustrated in Fig. 10, the PID control scheme performed poorly under non-ideal conditions, exhibiting noticeable deviations from the reference voltage, which underscores its limited capability to reject input-side disturbances. In contrast, the ISMC controller achieved better output regulation, offering moderate disturbance rejection. The proposed AMF-SMC scheme demonstrated the most robust performance, showing negligible deviation and a faster recovery throughout the test. These experimental results validate the superior adaptability and disturbance rejection capability of the AMF-SMC, making it a highly suitable solution for applications subject to unpredictable input supply variations.

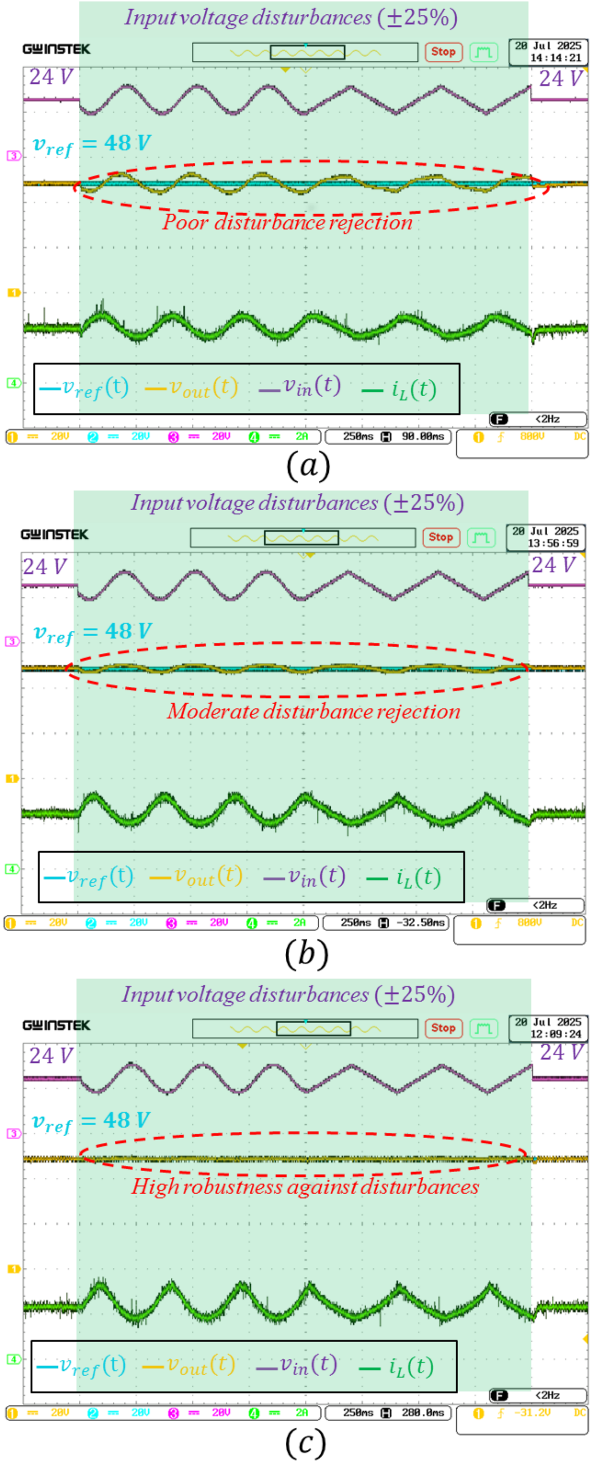

Fig. 10. Experimental results: under input voltage disturbances: (a) PID, (b) ISMC, (c) Proposed AMF-SMC

5 Conclusion

An adaptive model-free sliding mode control (AMF-SMC) scheme for DC–DC boost converters has been proposed, combining the ULM framework with SMC. The method achieves accurate voltage regulation under parameter variations and disturbances, while the adaptive gain mechanism mitigates chattering without requiring disturbance bounds. Furthermore, total system dynamics are well estimated in real-time using the TDE technique. Stability of the closed-loop system is proven via Lyapunov analysis. Experimental results under reference changes, load steps, and input voltage disturbances showed faster response, negligible overshoot, and superior disturbance rejection compared to PID and ISMC controllers, confirming the method's robustness for practical applications such as renewable energy and electric vehicles.

Acknowledgement

This work was supported by the General Directorate of Scientific Research and Technological Development/Ministry of High Education and Scientific Research of Algeria (DGRSDT/MESRS).

References

[1] S.A. Gorji, H.G. Sahebi, M. Ektesabi, and A.B. Rad, "Topologies and Control Schemes of Bidirectional DC–DC Power Converters: An Overview", *IEEE Access*, vol. 7, pp. 117997–118019, 2019. doi: 10.1109/ACCESS.2019.2937239

[2] M. Forouzesh, Y.P. Siwakoti, S. Gorji, F. Blaabjerg, and B. Lehman, "Step-Up DC–DC Converters: A Comprehensive Review of Voltage-Boosting Techniques, Topologies, and Applications", *IEEE Transactions on Power Electronics*, vol. 32, no. 12, pp. 9143–9178, 2017. doi: 10.1109/TPEL.2017.2652318

[3] Z. Chen, W. Gao, J. Hu, and X. Ye, "Closed-Loop Analysis and Cascade Control of a Nonminimum Phase Boost Converter", *IEEE Transactions on Power Electronics*, vol. 26, no. 4, pp. 1237–1252, 2010. doi: 10.1109/TPEL.2010.2070808

[4] R. Errouissi, A. Al-Durra, and S.M. Muyeen, "A Robust Continuous-Time MPC of a DC–DC Boost Converter Interfaced with a Grid-Connected Photovoltaic System", *IEEE Journal of Photovoltaics*, vol. 6, no. 6, pp. 1619–1629, 2016. doi: 10.1109/JPHOTOV.2016.2598271

[5] R. Yoganathan, J. Venkatesan, T.V. Narmadha, and I. William Christopher, "Performance Comparison of a DC–DC Boost Converter with Conventional and Non-Linear SMC Controller in Dual Loop Structure", *Electrical Power Components and Systems*, pp. 1–16, 2024. doi:10.1080/15325008.2024.2340744

[6] A. Kihal, F. Krim, A. Laib, B. Talbi, and H. Afghoul, "An Improved MPPT Scheme Employing Adaptive Integral Derivative Sliding Mode Control for Photovoltaic Systems under Fast Irradiation Changes", *ISA Transactions*, vol. 87, pp. 297–306, 2019. doi: 10.1016/j.isatra.2018.11.020

[7] S. Zheng, M. Qi, Y. Shu, Y. Wang, and J. Lang, "Non-Singular Terminal Sliding Mode Control Strategy for DC/DC Boost Converter System Using a Finite-Time Convergent Observer", *IET Power Electronics*, vol. 15, no. 16, pp. 1868–1876, 2022. doi: 10.1049/pel2.12354

[8] Y. Li, Z. Zhang, and R. Kennel, "A Full State-Variable Predictive Control of Bidirectional Boost Converters with Guaranteed Stability", *the 22nd European Conference on Power Electronics and Applications (EPE'20 ECCE Europe)*, 2020. doi:10.23919/EPE20ECCEEurope43536.2020.9215879

[9] M.M. Mardani, M.H. Khooban, A. Masoudian, and T. Dragicevic, "Model Predictive Control of DC–DC Converters to Mitigate the Effects of Pulsed Power Loads in Naval DC Microgrids", *IEEE Transactions on Industrial Electronics*, vol. 66, no. 7, pp. 5676–5685, 2019. doi:10.1109/TIE.2018.2877191

[10] M.E. Albira and M.A. Zohdy, "Adaptive Model Predictive Control for DC–DC Power Converters with Parameters' Uncertainties", *IEEE Access*, vol. 9, pp. 135121–135131, 2021. doi:10.1109/ACCESS.2021.3113299

[11] L. Po, L. Ruiyu, S. Tianying, Z. Jingrui, and F. Zheng, "Composite Adaptive Model Predictive Control for DC–DC Boost Converters", *IET Power Electronics*, vol. 11, no. 10, pp. 1706–1717, 2018. doi:10.1049/iet-pel.2017.0835

[12] J. Wang, W. Luo, J. Liu, and L. Wu, "Adaptive Type-2 FNN-Based Dynamic Sliding Mode Control of DC–DC Boost Converters", *IEEE Transactions on Systems, Man, and Cybernetics: Systems*, vol. 51, no. 4, pp. 2246–2257, 2019. doi:10.1109/TSMC.2019.2911721

[13] T. Qie, X. Zhang, C. Xiang, Y. Yu, H.H. Iu, and T. Fernando, "A New Robust Integral Reinforcement Learning Based Control Algorithm for Interleaved DC/DC Boost Converter", *IEEE Transactions on Industrial Electronics*, vol. 70, no. 4, pp. 3729–3739, 2022. doi: 10.1109/TIE.2022.3179558

[14] Y. Wei, H. Young, D. Ke, F. Wang, and J. Rodríguez, "Model-Free Predictive Current Control Using Extended Affine Ultra-local for PMSM Drives", *IEEE Transactions on Industrial Electronics*, vol. 71, no. 7, pp. 6719–6729, 2023. doi: 10.1109/TIE.2023.3314914

[15] X. Yuan, Y. Zuo, Y. Fan, and C.H. Lee, "Model-Free Predictive Current Control of SPMSM Drives Using Extended State Observer", *IEEE Transactions on Industrial Electronics*, vol. 69, no. 7, pp. 6540–6550, 2021. doi:10.1109/TIE.2021.3095816

[16] H. Zhang, H. Li, J. Mao, C. Pan, and Z. Luan, "Model-Free Control of Single-Phase Boost AC/DC Converters", *IEEE Transactions on Power Electronics*, vol. 37, no. 10, pp. 11828–11838, 2022. doi: 10.1109/TPEL.2022.3176937

[17] O. Babayomi, Z. Zhang, and Z. Li, "Model-Free Predictive Control of DC–DC Boost Converters: Sensor Noise Suppression with Hybrid Extended State Observers", *IEEE Transactions on Power Electronics*, vol. 39, no. 1, pp. 245–259, 2023. doi:10.1109/TPEL.2023.3321070

[18] M. Fliess and C. Join, "Model-Free Control", *International Journal of Control*, vol. 86, no. 12, pp. 2228–2252, 2013. doi:10.1080/00207179.2013.810345

[19] S. Ahmad and A. Ali, "Active Disturbance Rejection Control of DC–DC Boost Converter: A Review with Modifications for Improved Performance", *IET Power Electronics*, vol. 12, no. 8, pp. 2095–2107, 2019. doi: 10.1049/iet-pel.2018.5767

[20] G. Pereira das Neves and B. Augusto Angélico, "Model-Free Control of Mechatronic Systems Based on Algebraic Estimation", *Asian Journal of Control*, vol. 24, no. 4, pp. 1575–1584, 2022. doi:10.1002/asjc.2596

[21] F. Bento, I. Jlassi, and A.J.M. Cardoso, "Model-Free Predictive Control of Interleaved DC-DC Converters based on Ultra-Local Model with Constant Switching Frequency", *the IEEE Energy Conversion Congress and Exposition (ECCE)*, Oct. 2021. doi: 10.1109/ECCE47101.2021.9595318

[22] S. Han, H. Wang, and Y. Tian, "Model-Free Based Adaptive Nonsingular Fast Terminal Sliding Mode Control with Time-Delay Estimation for a 12 DOF Multi-Functional Lower Limb Exoskeleton", *Advances in Engineering Software*, vol. 119, pp. 38-47, 2018. doi:10.1016/j.advengsoft.2018.01.004

[23] H. Wang, Y. Xuefei, T. Yang, G. Zheng, and N. Christov, "Model-Free Based Terminal Sliding Mode Control of Quadrotor Attitude and Position", *IEEE Transactions on Aerospace and Electronic Systems*, vol. 52, no. 5, pp. 2519–2528, 2016. doi:10.1109/TAES.2016.150303

[24] C.E. Boudjedir, M. Bouri, and D. Boukhetala, "An Enhanced Adaptive Time Delay Control-Based Integral Sliding Mode for Trajectory Tracking of Robot Manipulators", *IEEE Transactions on Control Systems Technology*, vol. 31, no. 3, pp. 1042–1050, 2023. doi:10.1109/TCST.2022.3208491

[25] K. Zhao, W. Liu, T. Yin, R. Zhou, and W. Dai, "Model-Free Sliding Mode Control for PMSM Drive System Based on Ultra-Local Model", *Energy Engineering: Journal of the Association of Energy Engineers*, vol. 119, no. 2, pp. 767, 2022. doi:10.32604/EE.2021.018617

[26] J. Baek, S. Cho, and S. Han, "Practical Time-Delay Control with Adaptive Gains for Trajectory Tracking of Robot Manipulators", *IEEE Transactions on Industrial Electronics*, vol. 65, no. 7, pp. 5682–5692, 2018. doi:10.1109/TIE.2017.2782238

[27] J. Baek, W. Kwon, B. Kim, and S. Han, "A Widely Adaptive Time-Delayed Control and Its Application to Robot Manipulators", *IEEE Transactions on Industrial Electronics*, vol. 66, no. 7, pp. 5332–5342, 2019. doi:10.1109/TIE.2018.2869347

Abbes Kihal received the B.S., M.S., and Ph.D. degrees in electronics and industrial control from the University Ferhat Abbas of Setif, Algeria, in 2012, 2014, and 2019, respectively. He is currently an Associate Professor with the University of Science and Technology Houari Boumediene. His research interests include new converter topologies, control of power converters, reliability of power electronic systems, and renewable energy sources.

Chems Eddine Boudjedir received the M.Sc. and Ph.D. degrees in control engineering from the École Nationale Polytechnique, Algiers, Algeria, in 2015 and 2019 respectively. He is currently an Associate Professor with the University of Science and Technology Houari Boumediene, Algiers. His research interests include iterative learning control, sliding mode control, time delay control, disturbance observer, and robotics.

Billel Talbi received the B.Tech. (Hons.), M.Sc. (Hons.), and Ph.D. degrees in electronics engineering from the University of Ferhat Abbas Setif, Setif, in 2011, 2013, and 2018, respectively. He is currently an Associate Professor with the University Mohamed El Bachir El Ibrahimi of Bordj Bou Arreridj. His current research interests include control of power converters, power conversion techniques, and renewable energy systems.

Abdeslem Sahli received the Engr. (Hons.), Mag. (Hons.), and D.Sc. degrees in electronics engineering from the University Ferhat Abbas of Setif-1, Setif, Algeria, in 2009, 2012, and 2021 respectively. He is currently an Assistant Professor with the University Mohamed El Bachir El Ibrahimi of Bordj Bou Arreridj. His research interests include power quality, nonlinear control, advanced control strategies, multilevel inverters, new converter topologies, reliability of power electronic systems, and renewable energy conversion.

Abdelbasset Krama (Member, IEEE) received his B.Sc. and M.Sc. degrees in electrical engineering from Kasdi Merbah University, Algeria, in 2013 and 2015, and his Ph.D. from El Oued University, Algeria, in 2019. From 2018 to 2022, he was a researcher at Texas A&M University at Qatar, working on smart grid projects. He is currently a scientist at the Qatar Environment and Energy Research Institute (QEERI), Doha, Qatar. His research focuses on renewable energy conversion, microgrid control, and smart grid technologies.

Received 17 December 2025